04

Solar VUV telescope for nanosatellites

© S.V. Kuzin,[1,2] S.A. Bogachev,[3,4] N.F. Erkhova,[3] A.A. Pertsov,[2,3,4] I.P. Loboda,[3] A.A. Reva,[3] A.A. Kholodilov,[3] A.S. Ulyanov,[3] A.S. Kirichenko,[2,3,4] I.V. Malyshev,[5,6] A.E. Pestov,[5,6] V.N. Polkovnikov,[5] M.N. Toropov,[5,6] N.N. Tsybin,[5] N.I. Chkhalo,[5] V.A. Kryukovskiy,[7] V.N. Gorev,[8] A.A. Doroshkin,[8] A.M. Zadorozhniy,[8] V.Yu. Prokop'ev[8]

[1] Shubnikov Institute of Crystallography „Crystallography and Photonics" Russian Academy of Sciences,
119333 Moscow, Russia
[2] Terrestrial Physics Of Siberian Branch Of Russian Academy Of Sciences (ISTP SB RAS),
664033 Irkutsk, Russia
[3] Lebedev Physical Institute, Russian Academy of Sciences,
119991 Moscow, Russia
[4] Samara National Research University,
443086 Samara, Russia
[5] Institute of Physics of Microstructures, Russian Academy of Sciences,
607680 Nizhny Novgorod, Russia
[6] „Interoptics", Ltd.,
603087 Nizhny Novgorod, Russia
[7] Joint Company „Research and Production Corporation „Space Monitoring Systems, Information & Control and Electromechanical Complexes"named after A.G. Iosifian",
107078 Moscow, Russia
[8] Novosibirsk State University,
630090 Novosibirsk, Russia
e-mail: kirichenkoas@lebedev.ru

Received April 21, 2021
Revised April 21, 2021
Accepted April 21, 2021

Within the Universat program, a set of solar vacuum ultraviolet (VUV) telescopes has been developed for deployment on 6U nanosatellites. Telescopes are designed to get images of the solar corona. The spectral ranges of observations is considered, the characteristics of the nanosatellite from the point of view of the observations feasibility are opmized, the optical scheme of the telescope and VUV multilayer mirrors coatings and thin-film filters are modelled.

Keywords: Nanosatellite, VUV, telescope, solar corona.

DOI: 10.21883/TP.2022.13.52216.115-21

Introduction

Despite the existing limitations compared to full-sized space vehicles, nanosatellites become increasingly popular platform for applied and basic space studies. In the area of solar physics the series of experiments on studying the integral X-ray radiation of corona in a range of $\sim 0.5-30$ keV (MinXSS [1], „Yarilo"[2]) was performed, that showed the possibility of carrying over the part of applied studies to nanosatellites. At the same time the images of solar corona in vacuum ultraviolet (VUV) spectrum range are required for both applied and basic studies. Despite the fact that telescopes of VUV range are complex astro-space tools, they can be adapted for deployment on relatively small nanosatellite platforms with limited resources. Such projects are currently actively studied in leading spacefaring nations [3].

1. Spectral ranges of coronal plasma observation using space telescopes

Currently there are several spectral ranges of corona registration, that are the most in-demand for scientific and applied studies and mainly characterized by temperature of the registered solar plasma.

The coldest plasma range, transition layer, corresponds to temperatures of 20–100 thous. degrees. Transition layer is located directly above solar chromosphere and characterized by small thickness. Plasma heating to coronal temperatures is happened exactly in it. To solve the essential tasks of solar physics the observations of this layer are interesting in terms of transport of energy and matter of their photosphere to corona, mechanism of plasma heating and structure and dynamics of „magnetic mat". In terms of space weather forecasting the transition layer is important for two reasons: coronal holes are well localized in it — the areas, that

are the sources of high-speed solar wind, and prominences, destruction of which can result in solar eruptive processes. Transition layer observation is usually performed in line HeII with wavelength of 30.4 nm (excitation temperature is 50–70 thous. degrees).

The second temperature layer — this is a solar corona itself with temperature from 500 thous. to 2 mln degrees. Plasma with such temperature occupies the most part of the corona. It is well structured, the main coronal structures are well localized in it: active areas, magnetic field flux tubes, coronal holes, etc. Eruptive emissions of coronal matter also primarily consist of this plasma. For fundamental solar physics and applied tasks the flashing processes, related to energy concentration in plasma of this temperature range, and eruptive processes dynamics are of the main interest. Usually, this plasma observation is performed in lines FeIX-FeXIII — the most intensive lines of VUV range of solar corona spectrum after HeII. The most intensive line of the mentioned ones is FeIX 17.1 nm.

The third temperature layer — this is a flashing plasma with temperature above 3 mln degrees. There is almost none of it in undisturbed corona and it appears only during flashing processes, localized in small areas. Despite the short time of this plasma existence and localization areas, where it appears, its observations are highly important for understanding the nature of flashes and forecasting their development. Flashing plasma is observed in lines of ions with high degree of ionization, for instance, MgXII, Fe XXII-XXV. At the same time all „hot“ lines in coronal plasma are strongly blended with colder lines. Therefore, the most popular range for flashes observing is near 13.2 nm, where several intensive lines FeXXIII-FeXIV are concentrated, while coronal lines are rather weak.

Thus, in terms of space weather forecasting and fundamental physics tasks solving the solar corona observations should be performed in several spectral ranges, corresponding to various temperature layers.

2. Nanosatellite „Norbi-2“

Under the program of small space vehicles launching „UniverSat“ of the State Corporation „Roscosmos“ [4] the launch of nanosatellite (small space vehicle, SSV) „Norbi-2“ with solar VUV telescope is planned at the end of 2021. „Norbi-2“ is developed based on nanosatellite „Norbi“ [5], successfully launched to the low earth orbit in September of 2020 and currently undergoing the flight tests. Nanosatellite „Norbi-2“ of 6U format ($300 \times 200 \times 100$ mm), as well as „Norbi“, is created based on ultra-small space vehicles platform of the Novosibirsk State University, compatible with CubeSat standard. Basic subsystems of the platform:

— power supply system (PSS);

— onboard radio complex (ORC) with onboard control system functions;

— position and orientation system (POS);

— payload interface module.

Power supply system (PSS) provides electric power for all nanosatellite subsystems. PSS tasks are solar energy transformation into electrical energy, energy accumulation and distribution between SSV subsystems, as per specified algorithm, as well as monitoring of current state of the system parameters. Maximum power generated by PSS is 30 W. Flight tests of „Norbi“ on Earth?s orbit confirmed the design parameters of PSS and built-in function logic [5], therefore „Norbi-2“ will be equipped with the similar power supply system without any significant changes.

The main tasks of onboard radio complex of „Norbi“ with onboard control system functions are:

— organization of SSV radio communication with ground control complex (GCC);

— control of SSV subsystems and payload as per autonomous algorithms or at the commands received from GCC;

— collection of data from SSV subsystems and payload and their transfer through radio channel to GCC;

— monitoring of SSV subsystems state and payload and transfer of information on their state to GCC.

Onboard radio complex of „Norbi“ works on carrier frequency of 436.7 MHz. Transmit power of ORC transmitter is regulated in a range from 0.1 to 4 W. The specific feature of ORC of „Norbi“ is application of communication in radio channel, along with conventional frequency-shift keying FSK of broadband modulation LoRa [5,6], originally developed for Internet of Things networks [7]. LoRa modulation allows to significantly increase the transmission range or decrease the transmission power, thus lowering the transmitter power consumption. LoRa modulation in satellite radio communication was used for the first time at „Norbi“ At transmitter power of 0.2 W and application of LoRa modulation the ORC of „Norbi“ provides transfer of data from orbit of 580 km height to the Earth with a rate of up to ~ 10 kbit/s. Maximum transfer rate at transmitter power of 4 W is ~ 38 kbit/s. For transfer of higher quantity of images from solar VUV telescope it is not enough. Therefore, for capacity increase of communication channel „satellite-Earth“ the transmitter module with power of 8 W at frequency of ~ 2.4 GHz is planned to be added to the onboard radio complex „Norbi-2“ In this case with the corresponding modernization of antenna complex of GCC and application of LoRa modulation the rate of transfer through radio channel will be up to 1 Mbit/s for orbits with height of up to ~ 600 km at all satellite visibility angles.

Sun and Earth direction sensors, three-axis magnetometer, angular rate sensor and accelerometer, as well as GLONASS receiver [5,8] are used in the position and orientation system (POS) of „Norbi“ nanosatellite as orientation sensors. All sensors are integrated into single small orientation module Sun-horizon sensor (SHS); there are 10 SHS modules overall on „Norbi“ surface. Magnetic control system, in which the final controlling element is the system, consisting of three magnetic coils, oriented along the principal axes of inertia of the nanosatellite, is used for satellite position stabilization. This rather simple magnetic control system

allows to solve the nanosatellite settling down after separation from carrier rocket and to orient it in relation to the Sun and the Earth. Accuracy of Sun direction determination by SHS sensor is $\pm 0.15^\circ$, while angular resolution is $\sim 0.01^\circ$ [8]. Magnetic control system of „Norbi“ combined with SHS sensor allows to orient the satellite in relation to the Sun with accuracy of $\sim 0.5^\circ$. To increase the satellite stabilization accuracy, required for solar VUV telescope operation, the system of reaction wheels will be added to the POS of „Norbi-2“ as the final controlling element [9]. Typical accuracy of orientation support of SSV of CubeSat class by such systems is $\sim 0.001^\circ$ [10].

Payload interface module is an unified interface module for random payloads connection to SSV platform.

3. Optical scheme of VUV telescope for nanosatellites

Selection of telescope optical scheme is conditioned by relatively small volume dedicated for payload on satellite. Considering the substantial power consumption of telescope, the necessity of relatively powerful transmission for downlink, presence of relatively precision orientation and stabilization systems, telescope deployment on CubeSat is possible only for nanosatellite of format bigger than 6U ($1U \sim 100 \times 100 \times 100$ mm). At the same time the maximum size along any axis should not exceed 300 mm, i.e. for nanosatellite the dimensions of 6U are $\sim 300 \times 200 \times 100$ mm [11]. Considering deployment of the satellite support systems, 3U can be provided for telescope, i.e. volume of $300 \times 100 \times 100$ mm. In this volume, beside optical elements, the electronic and mechanical modules of telescope should be located. Based on these restrictions the compact optical two-mirrors system, that is a modernized Ritchey-Chretien system, was designed. Telescope arrangement in such configuration is presented in Fig. 1.

Disadvantage of this scheme in terms of nanosatellite operation is relatively small number of illuminated solar panels, they occupy an area of 1 dm^2. In case of placing a telescope input window on „lateral“ side of the telescope this area increases to 5 dm^2. Therefore, the scheme with „breaking“ plane mirror on input was also examined (Fig. 2).

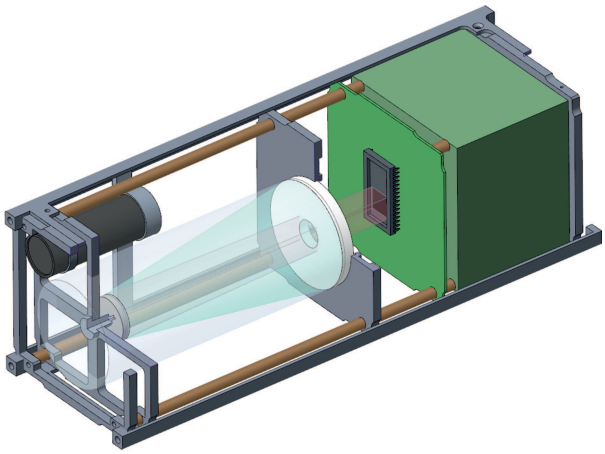

Figure 1. Arrangement of telescope with two-mirrors scheme.

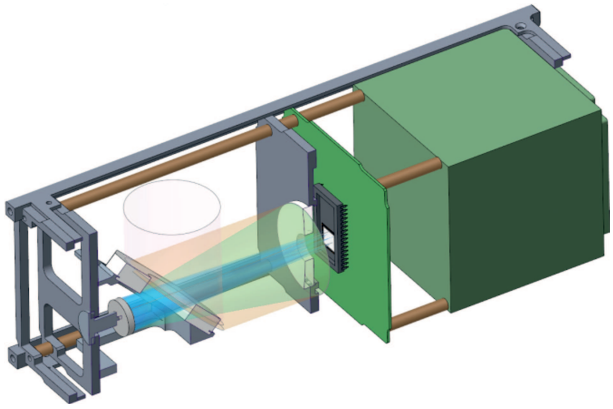

Figure 2. Arrangement of telescope with three-mirrors scheme.

Table 1. Main characteristics of CMOS-matrix

Parameters	Values
Format	2048×2048
Cell size, μm	6.5×6.5
Sensible area size, mm	13.3×133
Electronic shutter type	rolling

Table 2. Main optical characteristics of telescopes

Parameters	Two-mirrors scheme	Three-mirrors scheme
Field of view, °	1	1.4
Resolution in the center of field of view, arc. sec.	0.41	1.9
Resolution on the edge of field of view, arc. sec.	2.2	2.56
Vignetting, %	43	40

The main disadvantages of three-mirrors scheme are: increase of telescope weight, decrease of sensitivity by a factor of 5–10 depending on spectral range, higher requirements to mutual arrangement of optical elements.

In both optical schemes the application of CMOS-matrix with back-illumination GSENSE2020BSI-PS made by GPIXEL is planned (Table 1). The feature of this matrix is a minimum thickness of process and protecting layers of silicon oxide and nitride, that significantly improves efficiency of registration in VUV spectral range.

Characteristics of both schemes with application of a receiver based on GSENSE2020BSI-PS are presented in Table 2.

4. Multi-layer mirrors and VUV range filters for telescope

Optical systems based on multi-layer mirrors Mo/Si, traditionally used in the corresponding range, are effective for registration of lines of ions of flashing plasma near wavelength of 13.2 nm. Their peak reflection coefficient R can reach 68% [12]. At the same time the value of $\Delta\lambda$ (spectral width of reflection peak at half height) is 0.53 nm. This parameter influences the telescope spectral resolution.

In studies [13,14] it is shown, that, if required, to lower the value of $\Delta\lambda$ (increase spectral resolution of telescope) is possible by decreasing the molybdenum relative share in mirror period. However, it comes with decrease of R. Particularly, at $\Delta\lambda = 0.35$ nm $R = 53\%$.

Important advantage of Mo/Si mirrors is high timing stability of their reflecting characteristics. With long storage and use, if there are no factors, contaminating the surface, R and $\Delta\lambda$ remain on the same level for years.

Based on this pair of materials the multi-layer mirrors were created earlier to study the coronal plasma at a wavelength of 17.1 nm. For instance, mirrors of telescope TEREK [15] or telescope EIT of SOHO observatory [16]. However they were characterized by relatively small R (below 29%) and significant value of $\Delta\lambda$ (near 1.2 nm). Later optimized Mo/Si mirrors had $R = 54\%$, $\Delta\lambda = 0.875$ nm [17].

For better combination of high reflection and spectral selectivity the transition to mirrors based on aluminum, one of the most transparent materials in a range of wavelengths, exceeding 17.04 nm (L-aluminum absorption edge), is required. Such structures indeed allowed to improve spectral resolution, almost without loss of reflectivity. Thus, structures of Mo/Al/B_4C have $R = 55.5\%$, $\Delta\lambda = 0.875$ nm, while Mo/Al/SiC — $R = 53.4\%$, $\Delta\lambda = 0.76$ nm [18,19]. Zr/Al has the best resolution at comparable reflection coefficient: $R = 56\%$, $\Delta\lambda = 0.6$ nm [20].

Strategy of application of two relatively low-absorbing materials for mirrors creation is even better option. In study [21] aluminum and beryllium are proposed as such materials. Both materials have low absorption in the examined wavelength range, but there is a significant optical contrast between them (refractive differential). The same study suggests using amorphization property of thin barrier layer of silicon to reduce interlayer roughness between Al and Be. The resulting Al/Be/Si mirror had $R = 61\%$ and $\Delta\lambda = 0.4$ nm.

We optimized the parameters of the structure and obtained the mirror, spectral dependence of reflection coefficient of which is presented in Fig. 3. Peak reflection coefficient at wavelength of 17.1 nm was 62.5%, $\Delta\lambda = 0.3$ nm.

The same composition (Al/Be/Si) is reasonably to use for synthesis of mirrors intended for studying the transition layer at wavelength of 30.4 nm. In study [22] it is shown that Al/Be/Si structures have the best combination (for that range) of reflection coefficient and spectral selectivity: $R = 34.3\%$ and $\Delta\lambda = 1$ nm.

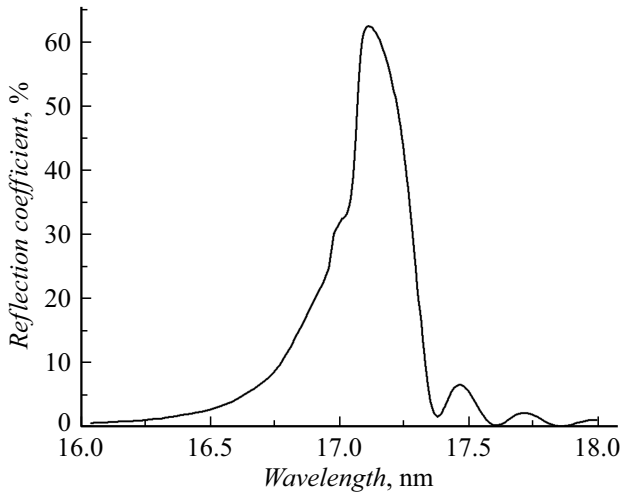

Figure 3. Spectral dependence of reflection coefficient of Al/Be/Si mirrors. Radiation incident angle of 2°. Measurements are performed at synchrotron BESSY-II.

Table 3. Multi-layer mirrors reflecting coatings characteristics

Registration channel	Structure	R, %	$\Delta\lambda$, nm
13.2 nm	Mo/Si with maximum R	68	0.53
13.2 nm	Mo/Si narrow-band	53	0.35
17.1 nm	Al/Be/Si	62.5	0.3
30.4 nm	Al/Be/Si	34.3	1

In study [14] the timing stability of reflecting characteristics of Al/Be/Si multi-layer structures was studied. It is shown, that within at least 20 months they do not decline.

Table 3 includes multi-layer structures, that are proposed to use as reflecting coatings of solar observatory optical elements. Absorption film filters are usually used in solar telescopes of extreme ultraviolet (EUV) range for suppression of solar radiation in visible and infrared (IR) ranges. By means of selecting the filter composition of materials with low absorption in operating spectral range of telescope, the filter can transmit the radiation in EUV range and block the radiation with longer waves. It is natural to optimize composition and thickness of film filter, so it could transmit maximum useful signal in operating range and at the same time provide the required degree of suppression of radiation of visible and IR ranges.

For overlapping of spectral range of 13–35 nm the TESIS observatory [23] used the intercomplementary pair of multi-layer absorption filters of Zr/Si and Al/Si. Composition and structure of film filters provided the required level of light suppression (better than 10^6 in visible range) and high mechanical strength, required for the film filters to withstand the satellite with telescope delivery without damage. Level of radiation suppression in visible and IR ranges is mainly defined by metal thickness in filter, while silicon adds an

additional absorption in EUV range (especially, in its long-wave part). Hence it is obvious that the higher transmission coefficient in a range of 17–35 nm with maintaining the level of visible and IR radiation suppression can be achieved using homogeneous aluminum film. However, the multi-layer aluminum filter is weaker than Al/Si. Besides, as time passes, aluminum may oxidize to significant thickness, that is undesirable, since it lowers its transmission coefficient in EUV range.

In the later study [24], the use of protective coatings of $MoSi_2$ with nanometric thickness was proposed to improve strength and oxidation stability of Al filters. Since the coatings are thin, they contribute much less in absorption in EUV range, than in case of Si layers use, therefore at comparable optical and mechanical characteristics $MoSi_2$/Al/$MoSi_2$ filters outmatch the early used multi-layer (Al/Si) filters in terms of transmission coefficient. In case of Zr/Si filters the silicon contribution into transmission coefficient lowering is not so significant (due to proximity of transmission band of Zr/Si filter to L absorption edge of Si).

Thus, this project suggests to use Al and multi-layer Zr/Si filters. To increase the level of protection against oxidation, it is suggested to use protective coatings of $MoSi_2$, as well as in case of Zr/Si multi-layer filter.

Fig. 4 shows design transmission coefficients for the following film filters:

1) $MoSi_2$ — 3 nm, Al — 150 nm, $MoSi_2$ — 3 nm;

2) $MoSi_2$ — 3 nm, (Zr — 3 nm/Si — 1 nm)·50, $MoSi_2$ — 3 nm.

Design transmission coefficients of film filters at wavelengths, corresponding to telescope registration channels, are: $T(13.2\,\text{nm}) = 49\%$, $T(17.1\,\text{nm}) = 63\%$, $T(30.4\,\text{nm}) = 31\%$.

The selected film thickness provides the required level of visible light suppression (better than 10^6).

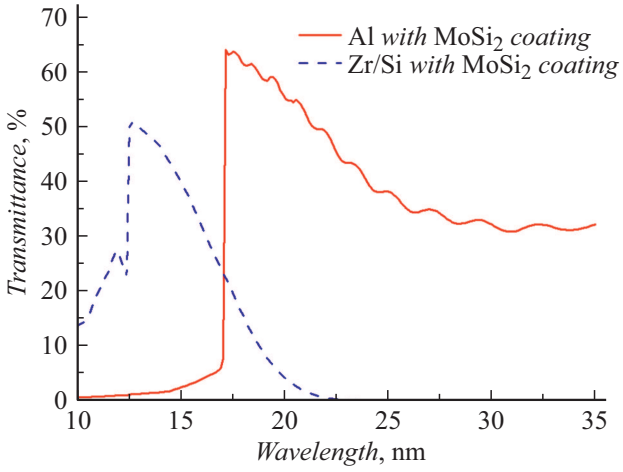

Figure 4. Design base transmission spectra of Zr/Si and Al film filters with protective $MoSi_2$ coatings at normal incidence. During calculations the optical constants from CXRO database were used [25].

Conclusion

The possibility of small telescopes creation for getting the VUV images of solar corona for nanosatellites is demonstrated. Development of these tools is suggested to perform under Roscosmos Universat program in 2021–2025. The nearest launch of „Norbi“ space vehicle with VUV telescope of a range of 17.1 nm is planned at the end of 2021.

Funding

The study was performed with support of the Ministry of Science and Higher Education during works performing under the Government Task of FSRC „Crystallography and Photonics“ of RAS, LPI, ISTP SB RAS and IPM RAS.

The study was partially performed under the project of FSSS-2020-0018, funded from the means of the Government Task for winners of contest among scientific laboratories of educational organization for higher education, under the jurisdiction of the Ministry of Education and Science of Russia.

Conflict of interest

The authors declare that they have no conflict of interest.

References

[1] J.P. Mason, T.N. Woods, A. Caspi, P.C. Chamberlin, C. Moore, A. Jones, R. Kohnert, X. Li, S. Palo, S.C. Solomon. J. Spacecraft Rockets, **53** (2), 328 (2016).

[2] N.V. Goncharov, M.Yu. Koretsky, V.I. Mayorova, V.G. Melnikova, N.A. Nerovnyj, D.A. Rachkin, S.M. Tenenbaum, E.D. Timakova, K.A. Frolov, I.V. Yastrebova, S.A. Bogachev, S.Yu. Dyatkov, A.S. Kirichenko, S.V. Kuzin, A.A. Pertsov. Kosmonavtika i raketostroenie, **1** (100), 69 (2018).

[3] J.P. Mason, Ph.C. Chamberlin1, D. Seaton J. Burkepile, R. Colaninno, K. Dissauer, F.G. Eparvier, Y. Fan, S. Gibson, A.R. Jones, C. Kay, M. Kirk, R. Kohnert, W.D. Pesnell, B.J. Thompson, A.M. Veronig, M.J. West, D. Windt, T.N. Woods. J. Space Weather Space Clim., **11** (20), (2021).

[4] Electronic source. Available at: https://www.roscosmos.ru/23836/

[5] V.Yu. Prokopyev, S.S. Bakanov, V.K. Bodrov, E.N. Chernodarov, A.A. Doroshkin, V.N. Gorev, A.Yu. Kolesnikova, A.S. Kozlov, O.N. Kus, A.V. Melkov, A.A. Mitrokhin, A.A. Morsin, A.E. Nazarenko, I.V. Neskorodev, A.V. Pelemeshko, Yu.M. Prokopyev, D.A. Romanov, A.M. Shilov, M.V. Shirokih, A.A. Sidorchuk, A.S. Styuf, A.M. Zadorozhny. J. Phys.: Conf. Ser. (2021, in press).

[6] A. Doroshkin, A. Zadorozhny, O. Kus, V. Prokopyev, Yu. Prokopyev. IEEE Access, **7**, 75721 (2019). DOI: 10.1109/ACCESS.2019.2919274

[7] C. Goursaud, J.-M. Gorce. EAI Endorsed Trans. Internet Things, **15** (1), e3 (2015). DOI: 10.4108/eai.26-10-2015.150597

[8] A. Pelemeshko, A. Kolesnikova, A. Melkov, V. Prokopyev, A. Zadorozhny. IOP Conf. Ser.: Mater. Sci. Eng., **734**, 012012 (2020). DOI: 0.1088/1757-899X/734/1/012012
[9] V.N. Vasiliev. *Sistemy orientatsii kosmicheskikh apparatov* (FGUP „NPP VNIIEM“, M., 2009) (in Russian).
[10] Z. Ismail, R. Varatharajoo. Adv. Space Res., **45**, 750 (2010). DOI: 10.1016/j.asr.2009.11.004
[11] CDS. 6UCubeSatDesignSpecification. Rev. Provisional. California Polytechnic State University, 2016.
[12] A.E. Yakshin, R.W.E. van de Kruijs, I. Nedelcu, E. Zoethout, E. Louis, F. Bijkerk, H. Enkisch, S. Müllender. Proc. SPIE, **6517**, 65170I (2007). DOI: 10.1117/12.711796
[13] S.A. Bogachev, N.I. Chkhalo, S.V. Kuzin, D.E. Pariev, V.N. Polkovnikov, N.N. Salashchenko, S.V. Shestov, S.Y. Zuev. Appl. Opt., **55** (9), 2126 (2016). doi.org/10.1364/AO.55.002126
[14] N. Chkhalo, A. Lopatin, A. Nechay, D. Pariev, A. Pestov, V. Polkovnikov, N. Salashchenko, F. Schäfers, M. Sertsu, A. Sokolov, M. Svechnikov, N. Tsybin, S. Zuev. J. Nanosci. Nanotechnol., **19**, 546 (2019).
[15] A. Ignatiev, N. Kolachevsky, V. Korneev, V. Krutov, S. Kuzin, A. Mitrofanov, A. Pertsov, E. Ragozin, V. Slemzin, I. Tindo, I. Zhitnik. Proc. SPIE, **3406**, 20 (1998).
[16] J.-P. Delaboudinière, G.E. Artzner, J. Brunaud, A.H. Gabriel, J.F. Hochedez, F. Millier, X.Y. Song, B. Au, K.P. Dere, R.A. Howard, R. Kreplin, D.J. Michels, J.D. Moses, J.M. Defise, C. Jamar, P. Rochus, J.P. Chauvineau, J.P. Marioge, R.C. Catura, J.R. Lemen, L. Shing, R.A. Stern, J.B. Gurman, W.M. Neupert, A. Maucherat, F. Clette, P. Cugnon, E.L. Van Dessel. Solar Physics, **162** (1–2), 291 (1995).
[17] R. Soufli, D.L. Windt, J.C. Robinson, S.L. Baker, E. Spiller, F.J. Dollar, A.L. Aquila, E.M. Gullikson, B. Kjornrattanawanich, J.F. Seely, L. Golub. Proc. SPIE, **5901**, 590101 (2005). DOI: 10.1117/12.617370
[18] M.H. Hu, K. Le Guen, J.M. André, P. Jonnard, E. Meltchakov, F. Delmotte, A. Galtayries. Opt. Express, **18** (19), 20019 (2010). DOI: 10.1364/OE.18.020019
[19] E. Meltchakova, A. Ziani, F. Auchere, X. Zhang, M. Roulliay, S. De Rossi, Ch. Bourassin-Bouchet, A. Jérome, F. Bridou, F. Varniere, F. Delmotte. Proc. SPIE, **8168**, 816819 (2011). https://doi.org/10.1117/12.896577
[20] S.Yu. Zuev, V.N. Polkovnikov, N.N. Salashchenko, S.V. Kuzin. Bull. Russ. Acad. Sci.: Phys., **74** (1), 50 (2010).
[21] N.I. Chkhalo, D.E. Pariev, V.N. Polkovnikov, N.N. Salashchenko, R.A. Shaposhnikov, I.L. Stroulea, M.V. Svechnikov, Yu.A. Vainer, S.Yu. Zuev. Thin Solid Films, **631**, 106 (2017). https://doi.org/10.1016/j.tsf.2017.04.020
[22] V.N. Polkovnikov, N.N. Salashchenko, M.V. Svechnikov, N.I. Chkhalo. Phys. Usp., **63** (1) (2020).
[23] S.V. Kuzin, I.A. Zhitnik, S.V. Shestov, S.A. Bogachev, O.I. Bugaenko, A.P. Ignat'ev, A.A. Pertsov, A.S. Ulyanov, A.A. Reva, V.A. Slemzin, N.K. Sukhodrev, Yu.S. Ivanov, L.A. Goncharov, A.V. Mitrofanov, S.G. Popov, T.A. Shergina, V.A. Solov'ev, S.N. Oparin, A.M. Zykov. Sol. Syst. Res., **45**, 166 (2011).
[24] N.I. Chkhalo, M.N. Drozdov, S.A. Gusev, A.Ya. Lopatin, V.I. Luchin, N.N. Salashchenko, D.A. Tatarskiy, N.N. Tsybin, S.Yu. Zuev. Appl. Opt., **58** (1), 21 (2019). https://doi.org/10.1364/AO.58.000021 25.
[25] Electronic source. Available at: https://henke.lbl.gov/optical_constants/